# Modeling the effect of anti-scalant on CaCO$_3$ precipitation in continuous flow

## Dmitry Lisitsin, David Hasson[*], Raphael Semiat

*Rabin Desalination Laboratory, Grand Water Research Institute, Department of Chemical Engineering,*
*Technion–Israel Institute of Technology, Haifa 32000, Israel*
*Tel. +972 (4) 829-2936/2009; Fax +972 (4) 8295672; email: hasson@tx.technion.ac.il*

**ABSTRACT**

Scale inhibition by anti-scalants is known to involve blockage of active growth sites by adsorbed inhibitor molecules, but there is virtually no quantitative information on the kinetics of anti-scalant retarded precipitation. This paper presents a model integrating the process of anti-scalant adsorption on precipitated CaCO$_3$ particles with the kinetics of the ensuing retarded precipitation. Adsorption is analyzed according to the Langmuir, Freundlich and Langmuir–Freundlich models, and CaCO$_3$ precipitation is described by the commonly used surface reaction controlled model. The proposed model is validated by experimental data measured in a continuous flow precipitation system over a wide range of conditions.

*Keywords*: CaCO$_3$ precipitation; Anti-scalants; Scale inhibition; Adsorption isotherms; Kinetics

## 1. Introduction

Anti-scalants are commonly used to control scale formation in cooling water systems and in desalination applications. Their conspicuous advantage is that, when properly applied, an anti-scalant can suppress effectively scale formation at very low dosages (typically below 10 ppm) and hence, at an affordable cost.

Despite the widespread use of anti-scalants, there is very limited quantitative information on the inhibition mechanisms involved. Models that describe the effect of an inhibitor on the growth rate of a crystallizing particle generally assume that the retardation effect is achieved via its adsorption on active growth sites. Sawada et al. [1] studied the adsorption of inorganic phosphates and organic polyphosphonates on calcite surfaces. In most cases, the adsorption process could be adequately described by the Freundlich and the Langmuir isotherms.

Bliznakov and Nikolaeva [2] proposed the following model to describe the effect of inhibitor adsorption on the crystal growth rate:

$$\frac{v - v_\infty}{v_0 - v_\infty} = 1 - \theta = 1 - \frac{K_L \cdot C}{1 + K_L \cdot C} \tag{1}$$

where $\theta$ is the fractional degree of crystal surface coverage, $C$ is the concentration of the growth inhibiting impurity in the crystallizing solution and $K_L$ is the equilibrium constant of the Langmuir adsorption isotherm. The step velocity $v$ of a crystal face in the absence of an inhibiting impurity ($\theta = 0$) is $v_0$ and for full surface coverage ($\theta = 1$) it reaches a limiting value $v_\infty$. Reddy and Nancollas [3] correlated the effect of organic scale inhibitor on CaCO$_3$ precipitation kinetics using the above model with limited success.

Kubota and Mullin [4] modified the growth retardation expression based on the Langmuir isotherm by introducing an additional parameter $\alpha$, which represents the effectiveness of the inhibitor:

$$\frac{v}{v_0} = 1 - \alpha \cdot \left( \frac{K_L \cdot C}{1 + K_L \cdot C} \right) \tag{2}$$

---

*Corresponding author.

With a highly effective inhibitor of $\alpha > 1$, the step velocity is stopped at $\theta_{eq} < 1$ (incomplete coverage of the crystal surface). In the case of $\alpha = 1$, the velocity reaches zero just at $\theta_{eq} = 1$, and for a weak inhibitor of $\alpha < 1$, the step velocity never becomes zero even at $\theta_{eq} = 1$ (complete coverage) but approaches a limiting value. Eq. (2) enables better correlation of experimental data [5–7] as it is based on two fitting parameters, $K_L$ and $\alpha$, instead of the single parameter $K_L$ of the Langmuir expression. In a study of the retardation of the growth rate of $CaCO_3$ crystals in the presence of metallic impurities such as $Zn^{2+}$, $Pb^{2+}$ and $Cu^{2+}$, Hasson et al. [8] adopted the Langmuir–Freundlich adsorption isotherm [9]:

$$\frac{v}{v_0} = 1 - \frac{K_{L-F} \cdot C^{1/n}}{1 + K_{L-F} \cdot C^{1/n}} \tag{3}$$

Eq. (3), which also embodies two fitting parameters ($K_{L-F}$ and $n$), was found to provide very good correlation of a wide range of experimental data with values of $n$ in the narrow range of 0.50 to 0.83.

The assumption that inhibited growth rate of $CaCO_3$ crystals occurs by a rapid equilibrium adsorption process seems to hold for most reported literature data. However, in a study of $CaCO_3$ precipitation in a continuous stirred tank in the presence of sodium hexa-meta phosphate (SHMP), Hasson and Cornel [10] found that the rate of SHMP adsorption varied inversely to the square root of the residence time. This result indicated that adsorption of the anti-scalant on the precipitated particles was a diffusion-controlled process. A possible reason for this deviation from the generally accepted assumption of almost instantaneous adsorption is that the Hasson and Cornel study was conducted with unusually high super-saturation conditions of the feed solution ($Ca^{2+} = CO_3^{2-} = 2000$ ppm as $CaCO_3$) and with high inhibitor concentrations reaching 100 ppm.

## 2. Modeling the effect of anti-scalant on $CaCO_3$ crystallization kinetics

The kinetics of surface reaction controlled $CaCO_3$ precipitation is commonly described by the following equation [11–14]:

$$r_S = k_{RS} \cdot \left( \left[ Ca^{2+} \right] \cdot \left[ CO_3^{2-} \right] - K'_{sp} \right) \tag{4}$$

where $r_S$ is the precipitation rate per unit surface of precipitated particles, $k_{RS}$ is a surface based precipitation reaction constant and $K'_{sp}$ is the solubility product of $CaCO_3$. Since determination of particles mass concentration is easier than measurement of particles surface,

Eq. (4) is often defined alternatively on the basis of the mass of the precipitated seeds:

$$r_m = k_{Rm} \cdot \left( \left[ Ca^{2+} \right] \cdot \left[ CO_3^{2-} \right] - K'_{sp} \right) \tag{5}$$

where $r_m$ is the precipitation rate per unit mass of precipitated particles and $k_{Rm}$ is a mass based precipitation reaction constant. The calcium depletion, $\Delta Ca^{2+}$ [mol/L], in a well stirred continuous flow crystallizer is therefore related to particles surface and particles mass respectively by:

$$\frac{\Delta \left[ Ca^{2+} \right]}{\tau} = k_{RS} \cdot S_{CaCO_3} \cdot \left( \left[ Ca^{2+} \right] \cdot \left[ CO_3^{2-} \right] - K'_{sp} \right)$$
$$= k_{Rm} \cdot m_{CaCO_3} \cdot \left( \left[ Ca^{2+} \right] \cdot \left[ CO_3^{2-} \right] - K'_{sp} \right) \tag{6}$$

where $S_{CaCO_3}$ is the specific seeds area [m$^2$/L solution] and $m_{CaCO_3}$ is the seeds concentration [gr/L solution].

Retardation of $CaCO_3$ precipitation due to the presence of impurities, such as inhibiting metal ions or common anti-scalants, has been analyzed assuming equilibrium adsorption of the impurity on some of the active sites available for crystal growth [8]. The decrease in $CaCO_3$ precipitation rate is attributed to the occupation of a fraction $\theta$ of the crystal active growth sites by adsorbed impurity molecules.

The $CaCO_3$ precipitation rate constant $k_R^0$ is reduced to the value of $k_R$ in the presence of adsorbed anti-scant molecules according to the fraction $(1-\theta)$ of unoccupied growth sites:

$$\frac{k_R}{k_R^0} = 1 - \theta \tag{7}$$

The relation between $\theta$ and residual anti-scalant concentration $P_f$ [mg$_{AS}$/L] can be described by three alternate

Table 1
Equations defining $\theta$ and $k_R$ for the various adsorption models

| Adsorption model | Occupied growth sites fraction | Crystallization rate coefficient |
|---|---|---|
| Langmuir | $\theta = \dfrac{K_L \cdot P_f}{1 + K_L \cdot P_f}$ | $k_R = \dfrac{k_R^0}{1 + K_L \cdot P_f}$ |
| Freundlich | $\theta = \dfrac{k}{b} \cdot P_f^{\,n} = K_F \cdot P_f^{\,n}$ | $k_R = k_R^0 \cdot \left( 1 - K_F \cdot P_f^{\,n} \right)$ |
| Langmuir–Freundlich | $\theta = \dfrac{K_{L-F} \cdot P_f^{1/n}}{1 + K_{L-F} \cdot P_f^{1/n}}$ | $k_R = \dfrac{k_R^0}{1 + K_{L-F} \cdot P_f^{1/n}}$ |

adsorption models: Langmuir, Freundlich and Langmuir–Freundlich [9]. Table 1 summarizes the equations defining the occupied growth sites fraction θ and the reduced precipitation rate constant $k_R$ according to the three models.

## 3. Verification of the anti-scalant inhibition kinetic model

### 3.1. Experimental system and methods

Fig. 1 shows the continuous flow system used to study the effect of an anti-scalant on the rate of CaCO₃ crystallization. Crystallization experiments were conducted in a 21 L thermo-insulated crystallizer.

#### 3.1.1. Analytical techniques

Particle size distributions were measured using a Coulter LS230 instrument. Dissolved calcium concentration was determined according to ASTM standard method D 511, by EDTA titration, using Murexide as the indicator. The total Ca and Mg hardness was measured by EDTA titration, using Erichrome Black T as the indicator. Total alkalinity of the solution was determined according to ASTM standard method D 1067, by HCl titration to the end point of pH 4.3.

In the analysis of the phosphonate anti-scalant investigated in this work, free phosphate ion in solution was determined by the phosphorus reactive method (Hach method No. 8048) using the Hach spectro-photometer DR 2010. Total dissolved phosphate ion in solution was determined by the Acid Persulfate digestion method (HACH method No. 8190).

#### 3.1.2. Experimental routine

The feed tank solution was maintained at a sufficiently low pH level in order to avoid CaCO₃ precipitation. Precipitation conditions in the crystallizer were induced by increasing the pH in the intermediate vessel to a desired controlled level. Each experiment lasted for a period corresponding to at least 5 crystallizer retention times so as to ensure steady state conditions. Crystallizer solution composition (pH, Ca²⁺ concentration and total alkalinity) and particle size distribution were periodically measured during an experimental run.

### 3.2. Analysis of retarded crystallization

Analysis of retarded crystallization was carried out by experimental determination of both kinetic and adsorption parameters. Values of the reaction constants $k_R$ on both area and mass basis ($k_{Rs}$ and $k_{Rm}$) were extracted from
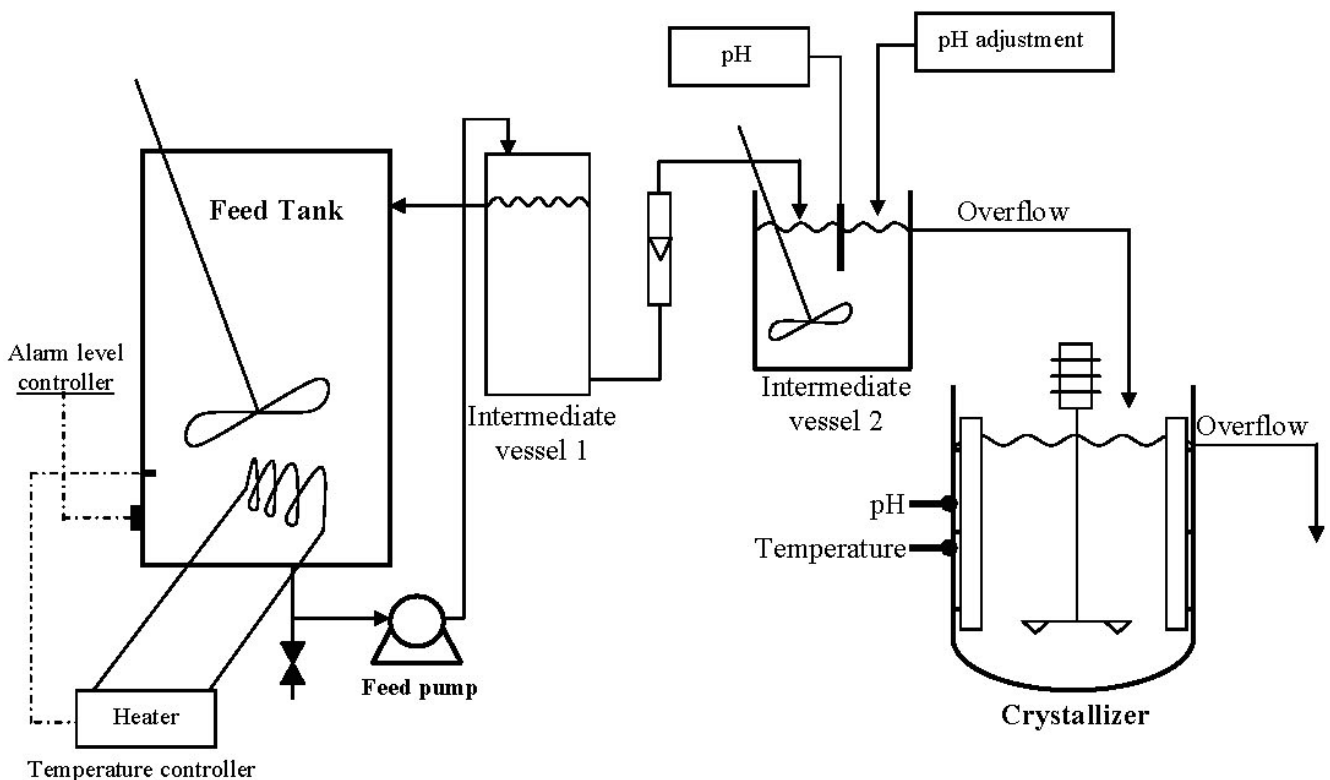


Fig. 1. Continuous flow CaCO₃ crystallization system.

measurements of the reaction conversion and of the specific surface area and mass of the seeds. The degree of anti-scalant adsorption was evaluated from measurements of anti-scalant concentrations in the solutions entering and leaving the crystallizer.

The fractional coverage of the crystal surface by adsorbed anti-scalant was characterized by determining both $\phi_{mass}$, the mass of anti-scalant adsorbed per unit mass of precipitated particles and $\phi_{area}$, the mass of anti-scalant adsorbed per unit surface of precipitated particles. The values of $\phi_{mass}$ and $\phi_{area}$, were obtained from:

$$\varphi_{mass} = \frac{P_0 - P_f}{m_{CaCO_3}} \left[ \frac{mg_{A/S}}{g_{CaCO_3}} \right] \tag{8}$$

$$\varphi_{area} = \frac{P_0 - P_f}{S_{CaCO_3}} \left[ \frac{mg_{A/S}}{m^2_{CaCO_3}} \right] \tag{9}$$

where $P_0$ [$mg_{A/S}$/L] is the feed concentration of the anti-scalant, $P_f$ [$mg_{A/S}$/L] is the residual anti-scalant concentration in the crystallizer, $m_{CaCO3}$ [$g_{CaCO3}$/L] is the mass concentration of the precipitated particles and $S_{CaCO3}$ [$m^2_{CaCO3}$/L] is the specific seeds surface area.

The measured values of $\phi_{mass}$ and $\phi_{area}$ are proportional to the fractional coverage $\theta$ of the precipitated particles by adsorbed anti-scalant molecules so that experimental values of the adsorption coefficients can be extracted from the expressions listed in Table 2.

### 3.3. Experimental results

Retarded $CaCO_3$ crystallization was studied using Permatreat PC 191-a phosphonate-based anti-scalant. The effect of anti-scalant on the kinetics of $CaCO_3$ crystallization was investigated by varying the feed anti-scalant concentration from 5 to 50 ppm and a retention time from 1 to 3 h. Table 3 shows the feed solution composition and the range of experimental parameters investigated.

Table 4 summarizes the experimental results; it displays values of the kinetic coefficients and of the anti-scalant adsorption on precipitated particles at various anti-scalant feed concentrations and at different retention times. It is seen that increase of the anti-scalant feed concentration leads to a substantial increase in the amount
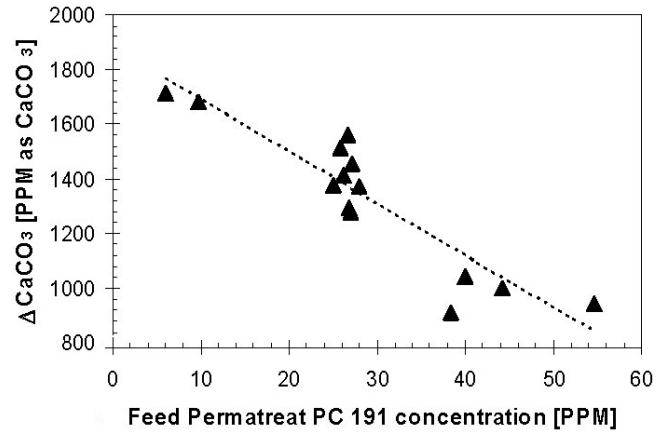


Fig. 2. Effect of Permatreat feed concentration on the degree of $CaCO_3$ precipitation at a retention time of 2 h.
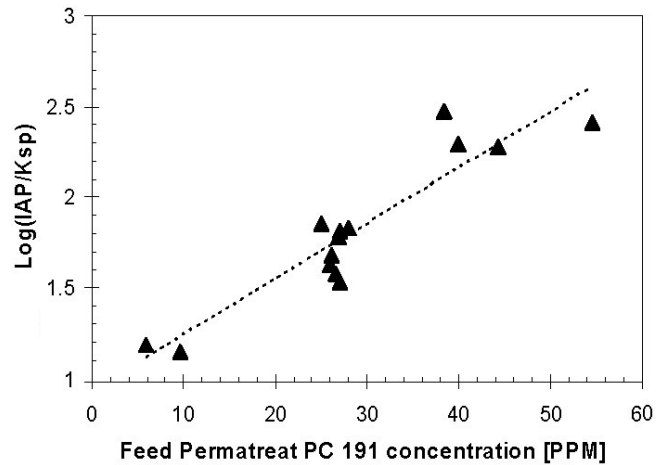


Fig. 3. Effect of Permatreat feed concentration on the residual supersaturation at a retention time of 2 h.

Table 2
Equations used to evaluate the adsorption coefficients

| | |
|---|---|
| Langmuir | $\varphi_{area}, \varphi_{mass} = b \cdot \theta = \dfrac{b \cdot K_L \cdot P_f}{1 + K_L \cdot P_f}$ |
| Freundlich | $\varphi_{area}, \varphi_{mass} = k \cdot P_f^n$ |
| Langmuir–Freundlich | $\varphi_{area}, \varphi_{mass} = b \cdot \theta = \dfrac{b \cdot K_{L-F} \cdot P_f^{1/n}}{1 + K_{L-F} \cdot P_f^{1/n}}$ |

Table 3
Solution composition and parameters investigated in the study of retarded $CaCO_3$ crystallization

| Ion | Concentration (ppm) | Parameter | Range |
|---|---|---|---|
| $Ca^{2+}$ | 680 | Retention time, h | 1–3 |
| $Na^+$ | 2800 | Permatreat feed concentration, ppm | 5–50 |
| $Cl^-$ | 3700 | Temperature, °C | 33 |
| $T_{Alk}$ | 2400 (as $CaCO_3$) | Agitation, rpm | 500 |

Table 4
Kinetic coefficients and adsorption levels of Permatreat PC 191

| Run no. | Retention time, h | Feed AS conc., ppm | Crystallization rate coefficients | | Anti-scalant adsorption | | Seeds concentration | |
|---|---|---|---|---|---|---|---|---|
| | | | $k_{RS}$ [L$^2$/mol·s·m$^2$] | $k_{Rm}$ [L$^2$/mol·s·g] | $\varphi_{mass}$ $\left[\dfrac{mg_{A/S}}{g_{CaCO3}}\right]$ | $\varphi_{area}$ $\left[\dfrac{mg_{A/S}}{m^2_{CaCO3}}\right]$ | $m_{CaCO3}$ $\left[\dfrac{g_{CaCO3}}{L}\right]$ | $S_{CaCO3}$ $\left[\dfrac{m^2_{CaCO3}}{L}\right]$ |
| 71 | 1 | 25 | 36 | 1.07 | 19.78 | 659 | 1.13 | 0.034 |
| 58 | | 25 | nm | 1.08 | 17.81 | nm | 1.12 | nm |
| 91 | | 25 | 41 | 1.2 | 16.96 | 574 | 1.39 | 0.041 |
| 92 | | 25 | 44 | 1.16 | 12.98 | 488 | 1.69 | 0.045 |
| 103 | | 10 | 69 | 2.86 | 3.91 | 94 | 1.90 | 0.079 |
| 51 | 2 | 25 | 36 | 1.04 | 11.89 | 414 | 1.85 | 0.053 |
| 52 | | 25 | 23 | 0.81 | 15.42 | 436 | 1.41 | 0.05 |
| 53 | | 25 | 34 | 0.92 | 9.59 | 354 | 2.44 | 0.066 |
| 57 | | 25 | nm | 0.71 | 14.68 | nm | 1.47 | nm |
| 65 | | 25 | 26 | 0.6 | 12.27 | 525 | 1.84 | 0.043 |
| 67 | | 10 | 100 | 3.82 | 4.72 | 122 | 1.81 | 0.07 |
| 68 | | 50 | 5.2 | 0.17 | 29.39 | 910 | 1.18 | 0.038 |
| 69 | | 5 | 121 | 4.45 | 3.47 | 94 | 1.41 | 0.052 |
| 70 | | 40 | 5.9 | 0.19 | 22.4 | 690 | 1.48 | 0.048 |
| 76 | | 40 | 5.4 | 0.16 | 27.1 | 882 | 0.98 | 0.03 |
| 80 | | 40 | 8.4 | 0.27 | 26.67 | 826 | 1.05 | 0.034 |
| 93 | 1.5 | 25 | 38 | 1.05 | 10.09 | 365 | 2.13 | 0.059 |
| 59 | 3 | 25 | nm | 0.45 | 7.86 | nm | 1.49 | nm |

Table 5
Best fit parameters based on alternate adsorption isotherms

| Model | Based on seeds area | Based on seeds mass |
|---|---|---|
| Langmuir | $K_L = 0.46 \left(\dfrac{L}{m^2_{CaCO3}}\right); b = 0.038 \left(\dfrac{mg_{A/S}}{m^2_{CaCO3}}\right)$ | $K_L = 0.5 \left(\dfrac{L}{mg_{A/S}}\right); b = 14 \left(\dfrac{mg_{A/S}}{g_{CaCO3}}\right)$ |
| Freundlich | $K_F = 10.7 \left(\dfrac{L}{m^2_{CaCO3}}\right)^{2.86}; \ n = 0.35$ | $K_F = 0.03 \left(\dfrac{L}{mg_{A/S}}\right)^{2.5}; \ n = 0.4$ |
| | $b = 0.032 \left(\dfrac{mg_{A/S}}{m^2_{CaCO3}}\right)$ | $b = 8.2 \left(\dfrac{mg_{A/S}}{g_{CaCO3}}\right)$ |
| Langmuir–Freundlich | $K_{L-F} = 0.19 \left(\dfrac{L}{mg_{A/S}}\right)^{0.625}; \ n = 0.625;$ | $K_{L-F} = 0.3 \left(\dfrac{L}{mg_{A/S}}\right)^{0.50}; \ n = 0.50$ |
| | $b = 0.017 \left(\dfrac{mg_{A/S}}{m^2_{CaCO3}}\right)$ | $b = 2.93 \left(\dfrac{mg_{A/S}}{g_{CaCO3}}\right)$ |

of adsorbed anti-scalant and decreases dramatically the CaCO$_3$ crystallization rate constant $k_R$.

Figs. 2 and 3 show the effect of anti-scalant feed concentration on the amount of precipitated CaCO$_3$ and on the residual supersaturation level. Increase of anti-scalant feed concentration is seen to reduce considerably the degree of CaCO$_3$ precipitation and to augment significantly the supersaturation level maintained in the crystallizer solution.

The data in Table 4 characterizing retarded crystalli-
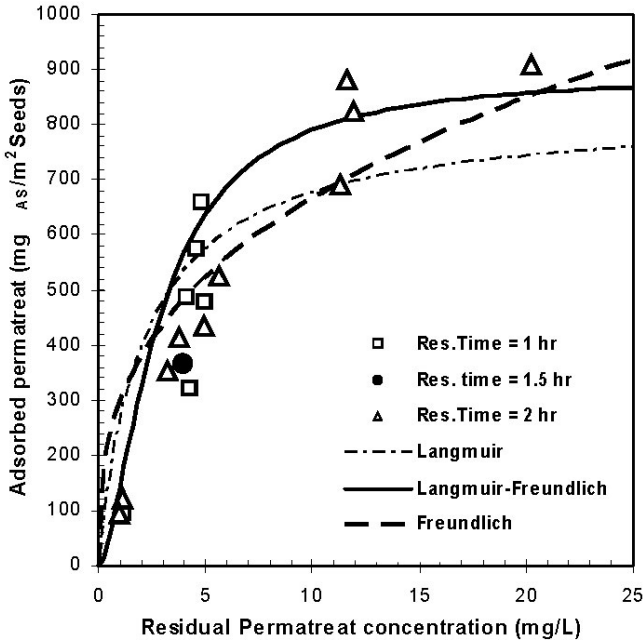
Fig. 4. Anti-scalant adsorption based on seeds area vs. residual anti-scalant concentration.
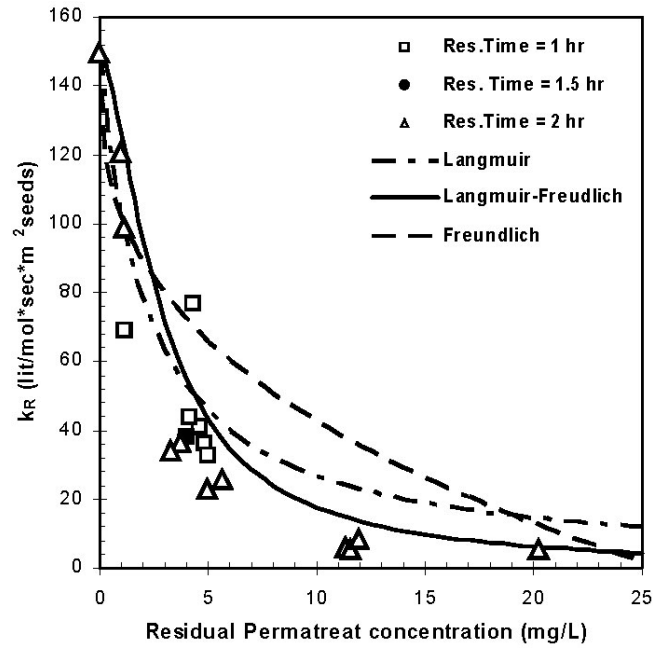


Fig. 5. Kinetic constant based on seeds area vs. residual anti-scalant concentration.
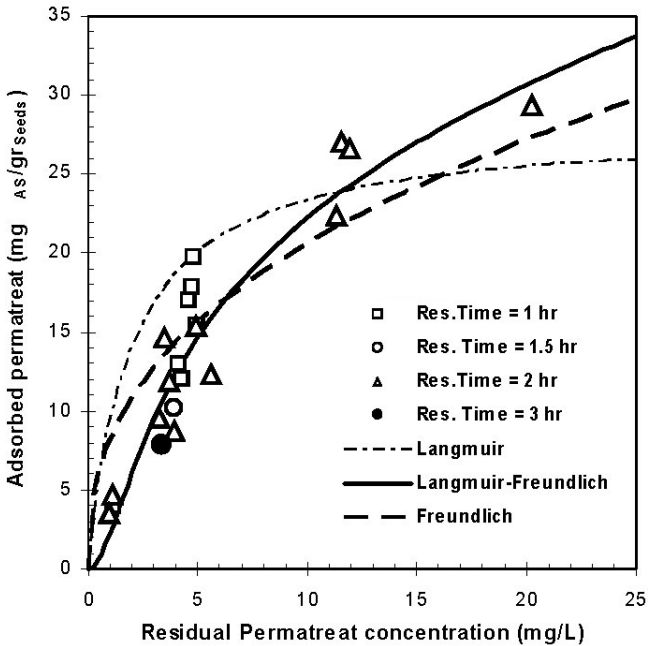


Fig. 6. Anti-scalant adsorption based on seeds mass vs. residual anti-scalant concentration.
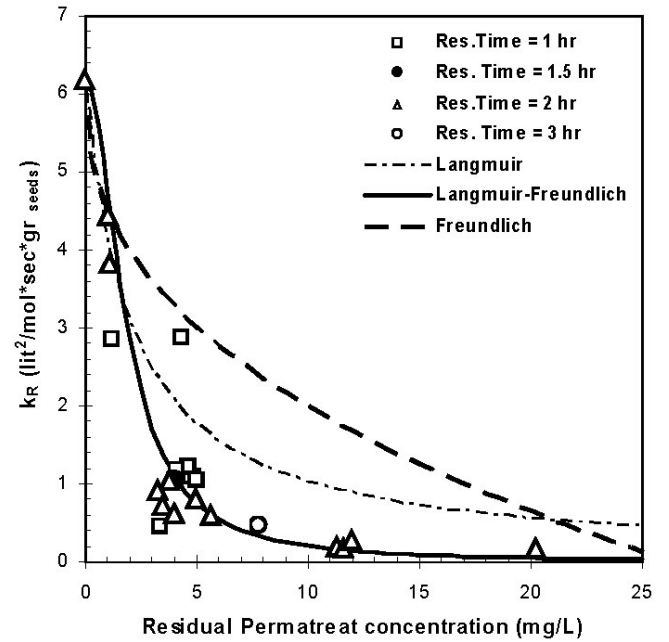


Fig. 7. Kinetic constant based on seeds mass vs. residual anti-scalant concentration.

zation of $CaCO_3$ by anti-scalant adsorption were correlated according to the three alternate adsorption models. Table 5 gives the best fit values of the kinetic coefficients and the adsorption coefficients listed in Table 2; these values were obtained by statistical regression of the experimental data, minimizing the sum of squares of the error (SSE). It is interesting to note that the values of $n =$ 0.625 and $n = 0.503$ of the model based on the Langmuir–Freundlich isotherm are in good agreement with values in the range of 0.5 to 0.83 reported by Hasson et al. [8] for $CaCO_3$ inhibition by trace metallic concentrations of various metal ions.

The fit of the data to the correlating models can be assessed by comparing the experimental results with
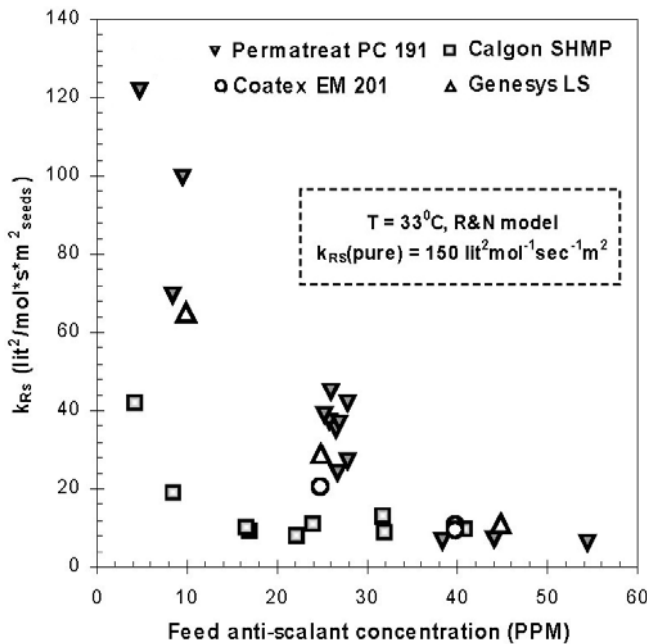
Fig. 8. Comparison of the kinetic rate coefficient $k_{Rs}$ induced by various anti-scalants.

calculated values based on the parameters listed in Table 5. Figs. 4 and 6 display the effect of residual anti-scalant concentration on the level of anti-scalant adsorption on the precipitated particles. Figs. 5 and 7 show the effect of anti-scalant concentration on the magnitude of the crystallization reaction kinetic coefficient $k_R$. It is seen that all adsorption models describe reasonably well the experimental trends. The best fit of both the adsorption and reaction constant data is obtained by the Langmuir-Freundlich model.

It may be also noted from Figs. 4 and 6 that the amounts of anti-scalant adsorbed on particles precipitated at different retention times extending from 0.5 to 3 h, all fall substantially on the same line. This result supports the hypothesis that the adsorption process is fast, justifying the assumption of equilibrium adsorption.

### 3.4. Comparison of inhibition effect of various anti-scalants

A comparison of the inhibited CaCO₃ crystallization rate coefficient induced by various anti-scalants was performed by determining values of $k_R$ as a function of anti-scalant inlet concentration. The comparison was carried out with four commercial anti-scalants: Permatreat PC 191, SHMP, Coatex EM 201 and Genesys LS. The experimental conditions were the same as listed in Table 3.

Fig. 8 compares values of the CaCO₃ crystallization rate coefficient, based on seeds area $k_{Rs}$, as a function of anti-scalant feed concentration of different anti-scalants. All commercial anti-scalants except SHMP are seen to exhibit a substantially similar inhibitory effect on the CaCO₃ rate coefficient. SHMP displayed the strongest inhibition effect, inducing a reduced crystallization rate by a factor of 4 to 5 at anti-scalant concentrations of 10 PPM. Another interesting observation is that, irrespective of the anti-scalant nature, all anti-scalants lead to the same asymptotic value of 6–12 L²·mol⁻¹·s⁻¹·m⁻² when the feed anti-scalant concentration exceeds 30 ppm. This phenomenon merits further investigation.

## 4. Conclusions

The major problems in the application of anti-scalants are that available products are largely shrouded in commercial secrecy and that the effects of operating parameters on inhibition effectiveness are largely unpredictable. The main contribution of this paper lies in providing quantitative data relating to the kinetics of CaCO₃ precipitation in the presence of anti-scalants.

## 5. Symbols

| | | |
|---|---|---|
| $b$ | — | Factor relating anti-scalant mass to occupied crystal area, $mg_{AS}/m^2_{CaCO3}$ or $mg_{AS}/g_{CaCO3}$ |
| $C$ | — | Anti-scalant concentration, $mg_{AS}/L$ |
| $K_L$ | — | Langmuir isotherm coefficient, $L/mg_{A/S}$ or $L/g_{CaCO3}$ |
| $K_F$ | — | Freundlich isotherm coefficient, $(L/m^2_{CaCO3})$ $1/n$ or $(L/mg_{AS})$ $1/n$ |
| $K_{L-F}$ | — | Langmuir–Freundlich isotherm coefficient, $(L/m^2_{CaCO3})n$ or $(L/mg_{AS})n$ |
| $k_R^0$ | — | CaCO₃ crystallization rate coefficient in the absence of inhibition, units of $k_{Rm}$ or $k_{Rs}$ |
| $k_R$ | — | CaCO₃ crystallization rate coefficient in the presence of inhibition, units of $k_{Rm}$ or $k_{Rs}$ |
| $k_{Rm}$ | — | CaCO₃ crystallization rate coefficient based on seeds mass, $L^2/mol\ s/g$ seeds |
| $k_{Rs}$ | — | CaCO₃ crystallization rate coefficient based on seed area, $L^2/mol\ s\ m^2$ |
| $K'_{sp}$ | — | Solubility product of CaCO₃ corrected for ionic strength, $[mol/L]^2$ |
| $m_{CaCO3}$ | — | Specific seeds mass, $g/L$ |
| $n$ | — | Power index in adsorption isotherms |
| $P_o$ | — | Feed anti-scalant concentration, $mg/L$ |
| $P_f$ | — | Residual anti-scalant concentration, $mg/L$ |
| $r_S$ | — | CaCO₃ crystallization rate based on seeds area, $mol/s\ m^2$ |
| $r_m$ | — | CaCO₃ crystallization rate based on seeds mass, $mol/s\ g$ seeds |
| $S_{CaCO3}$ | — | Specific seeds area, $m^2/L$ |
| $T_{Alk}$ | — | Total carbonate alkalinity, $eq./L$ |
| $v$ | — | Step velocity of a crystal face in the presence of an impurity, $m/s$ |

$v_0$ — Step velocity of a crystal face in a pure solution, m/s

$v_\infty$ — Limiting step velocity in impure solution, m/s

*Greek*

$\alpha$ — Effectiveness factor of the inhibiting impurity

$\theta$ — Fractional coverage of crystal growth sites

$\tau$ — Mean residence time of solution in crystallizer, h

$\phi_{mass}$ — Specific mass of the adsorbed anti-scalant, $mg_{A/S}/g$

$\phi_{area}$ — Specific area of the adsorbed anti-scalant, $mg_{A/S}/m^2$

## Acknowledgment

## References

[1]   K. Sawada, N. Abdel-Aal, H. Sekino and K. Satoh, Adsorption of inorganic phosphates and organic polyphosphonate on calcite, Dalton Trans., 3 (2003) 342–347.

[2]   R. Bliznakov and R. Nikolaeva, Kristall Tech., 2 (1967) 161 (cited in [4]).

[3]   M.M. Reddy and G.H. Nancollas, Calcite crystal growth inhibition by phosphonates, Desalination, 12 (1973) 61–73.

[4]   N. Kubota and J. W. Mullin, A kinetic model for crystal growth from aqueous solution in the presence of impurity, J. Crystal Growth, 152(3) (1995) 203–208.

[5]   J. Ulrich and S. Al-Jibbouri, The influence of impurities on crystallization kinetics of sodium chloride, Crystal Res. Technol., 36(12) (2001) 1365–1375.

[6]   M. Rauls, K. Bartosch, M. Kind, S. Kuch, R. Lacmann and A. Mersmann, The influence of impurities on crystallization kinetics—a case study on ammonium sulfate, J. Crystal Growth, 213(1/2) (2000) 116–128.

[7]   K-J Westin and A.C. Rasmuson, Crystal growth of aragonite and calcite in presence of citric acid, DTPA, EDTA and pyromellitic acid, J. Coll. Interf. Sci., 282(2) (2005) 359–369.

[8]   D. Hasson, R. Semiat, M. Ilevicky, D. Damiano and A. Sher, Inhibition of $CaCO_3$ scale deposition by trace concentrations of some common ions, Proc. AWWA Water Quality Conference, San Antonio, Texas, 2004.

[9]   C. Tien, Adsorption Calculations and Modeling, Butterworth–Heinemann, 1994.

[10]  D. Hasson and A. Cornel, Kinetics of $CaCO_3$ precipitation in the presence of SHMP, NACE Corrosion/2007, Science and Technology of Industrial Water Treatment Symposium, Nashville, Tennessee, Paper No. 07051, 2007.

[11]  G.H. Nancollas and M.M. Reddy, Crystallization of calcium carbonate. II: Calcite growth mechanism, J. Coll. Interf. Sci., 37(4) (1971) 824–830.

[12]  G.H. Nancollas and M.M. Reddy, Crystal growth kinetics of minerals encountered in water treatment processes, in: Aqueous Environmental Chemistry of Metals, A.J. Rubin, ed., Ann-Arbor Science, 1974, Chap. 6.

[13]  H.N.S. Wiechers, P. Sturrock and G.V.R. Marais, $CaCO_3$ crystallization kinetics, Water Res., 9 (1975) 835–845.

[14]  D. Hasson, H. Sherman and M. Biton, Prediction of calcium carbonate scaling rates, Proc. 6th Intern. Symp. on Fresh Water from the Sea, 2 (1978) 193–199.